

Research Article

Dynamic Characteristics and Mechanism of the Saturated Compacted Loess under Freeze-Thaw Cycles

Qian Wang ^{1,2}, Fuqiang Liu,^{1,2,3} Xiumei Zhong,^{1,2} Zhongnan Gao,^{1,2} Shouyun Liang,³ and Yuxin Liang³

¹Key Laboratory of Loess Earthquake Engineering, China Earthquake Administration & Gansu Province, 450 Donggang West Road, Lanzhou 730000, China

²Lanzhou Institute of Seismology, China Earthquake Administration, 450 Donggang West Road, Lanzhou, Gansu 730000, China

³Department of Civil Engineering and Mechanics, Lanzhou University, 222 Tianshui South Road, Lanzhou 730000, China

Correspondence should be addressed to Qian Wang; wangq0930@126.com

Received 7 July 2021; Revised 2 September 2021; Accepted 13 September 2021; Published 8 October 2021

Academic Editor: Zhongqiong Zhang

Copyright © 2021 Qian Wang et al. This is an open access article distributed under the Creative Commons Attribution License, which permits unrestricted use, distribution, and reproduction in any medium, provided the original work is properly cited.

To study the dynamic characteristics and mechanism of saturated loess after freeze-thaw cycles, a series of laboratory tests including freeze-thaw cycle tests, dynamic triaxial tests, and scanning electron microscope tests of the saturated remolded loess was conducted. The characteristics of the dynamic parameters of the saturated loess after different freeze-thaw cycles were discussed. The characteristics of the microstructure parameters changes were analyzed. The evolution process and mechanism of the microstructure of the remolded loess under freeze-thaw cycles were proposed. The results show that after different freeze-thaw cycles, the dynamic stress-dynamic strain curves of the saturated remolded loess conform to the hyperbolic model; however, the freeze-thaw cycle has a significant effect on the model parameter b . With the increase of freeze-thaw cycles, the dynamic shear modulus of saturated remolded loess first decreases and then increases, while the damping ratio is opposite. When saturated remolded loess experiences freeze-thaw cycles greater than four, its dynamic stability is better than that of saturated soil without freeze-thaw cycles. The dynamic stability reaches its peak after seven freeze-thaw cycles and is equivalent to that of saturated soil without freeze-thaw cycles after forty cycles. Combined with the results of the quantitative analysis of microstructure images, with the increase of the freeze-thaw cycles, the number of large and medium particles in the soil reduces, and the number of micros and small particles increases. The particle size tends to be uniform. The apparent porosity increases rapidly and then decreases sharply and tends to be stable after 4 freeze-thaw cycles. The pore and particle fractal dimensions continue to decrease. The probability of entropy increases first and then decreases. It is illustrated that the saturated loess has mainly experienced three steps under freeze-thaw cycles: (1) fracture and expansion of original skeleton cementation, (2) damage, crushing and aggregation of the particle, and (3) compaction and reorganization of soil structure. Besides, the saturation condition significantly accelerates the evolution process of the internal structure of the soil under freeze-thaw cycles. These lead to the strengthening effect of soil dynamic stiffness under long-term freeze-thaw cycles.

1. Introduction

Loess is a kind of special soil formed in an arid climate, which is widely distributed in seasonal frozen areas of Middle and Western China. Due to its special porous and weakly cemented structure, it has a high risk of disaster under external forces [1–3]. The freeze-thaw cycle as a special strong weathering effect can significantly change the structure and physical and mechanical properties of soil, which is easy to

lead to strength deterioration of soil and causes the destruction of various engineering infrastructure [4–6]. The physical and mechanical properties and structural behaviors of the soil change due to cryogenic actions in the freeze-thaw cycle. The interaction of confining pressure, freezing temperature, and freeze-thaw cycles has a significant impact on the strength of silty soil [7–12], as well as the nonlinear dynamic parameters and characteristics of seismic engineering [13, 14]. The main reason that causes the variation of the

static and kinetic behaviors of the soil during the freezing-thaw cycle is the changes in microstructure. The freezing-thaw condition causes the breaking and sliding of particles, as well as the rearrangement of the pore. However, the structural damage of the soil trends to stable with the increase of the freezing-thaw cycles [15–19].

The freeze-thaw cycle effect is mainly reflected as the phase change and migration effects of water in the soil [20, 21]. The initial moisture content of the soil has a significant impact on the physical and mechanical properties after the freeze-thaw cycle [22–24]. The cohesion of intact loess and remolded loess both decreased with the increase of the initial moisture content, while there is no obvious change rule in the internal friction angle in different freeze-thaw conditions [25, 26]. It can be seen from many discussions of the freeze-thaw cycles on the physical and mechanical properties and mechanism of unsaturated soil and achieved fruitful results. However, there are few researches on the physical and mechanical properties and microcosmic mechanism of saturated loess under the freeze-thaw cycle, especially for the dynamic behaviors [27]. Affected by the engineering behavior, groundwater, atmospheric rainfall, snowmelt, and the strong water sensitivity of loess, it is easy to cause the moisture content of unsaturated loess to increase sharply. The moisture content of the foundation soil often deviates from the initial design value and the dynamic features, resulting in uneven frost deformation of the building, which makes the foundation unable to operate normally or even damages it. Therefore, in this paper, intact loess samples were sampled in typical sites of Lanzhou City, which were located in the seasonal frost region of the Loess Plateau. After the sample was reshaped and saturated indoors, the high-low temperature test chamber was used to simulate the freeze-thaw cycle process to do different periods of freeze-thaw cycle tests. Then, the dynamic triaxial test was carried out. Combined with the results of the SEM microstructure test, the dynamic characteristics and microstructure changes of saturated loess affected by the freeze-thaw cycles were analyzed, which provides scientific evidence for frost heaving of loess subgrade and improvement of freezing soil in seasonal freezing areas and seismic damage prevention.

2. Samples and Testing Methods

2.1. Samples. The sample was collected from a loess site in Heping Town of Lanzhou City, the capital of Gansu Province in China. The loess soil was formed in the Late Pleistocene, and we collected all samples at an embedded depth of approximately 4.5 m. The exploration well was excavated manually in-site, and the original cube test block was taken from the wall of the well. The basic physical properties of loess samples were tested following the “Chinese standard for test methods of earthworks” (GB/T 50123-2019) [28], and the results are shown in Table 1 and Figure 1.

The maximum dry density of the tested loess was 1.71 g/cm^3 , and the optimum moisture content of the tested loess was 18.4% through the proctor compaction test. The moisture content of the prepared dry soil was modulated to the optimal moisture content and cured for 24 h, and

TABLE 1: Properties of loess samples.

Parameters	Value
Density	1.36 g/cm^3
Moisture	5.59%
Specific gravity	2.70
Plastic limit	15.9%
Liquid limit	24.1%
Plastic index	8.2

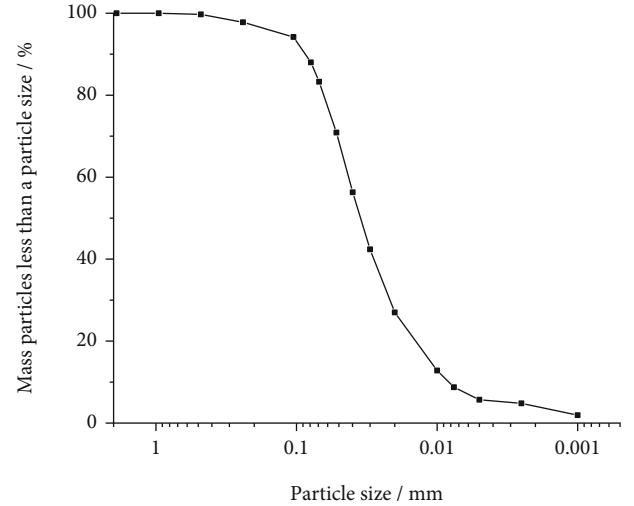


FIGURE 1: Particle size distribution of loess samples.

the soil sample was put into a cylindrical mold with an inside diameter of 50 mm. Figure 2(a) shows the sample was prepared by static pressure at both ends, and the size of the prepared sample was $\Phi 50\text{mm} \times 100 \text{ mm}$.

2.2. Testing Equipment and Methods

2.2.1. Sample Saturation. The prepared cylindrical remolding sample was put into the test cylinder, which was vacuumized first and then injected with water to saturate the soil sample. To ensure that the test sample is fully saturated, the pumping time is set to 5 hours. After pumping, the water inlet valve was opened. Due to the difference between the inside and outside atmospheric pressure, the distilled water automatically entered the saturation cylinder and the sample was completely submerged and then let stand still for 24 hours (Figure 2(b)) to make the sample reach a saturated state. The saturation degree of the soil sample after the test was 0.98.

2.2.2. Freeze-Thaw Cycle Test. An LK-120G programmable constant temperature and humidity test chambers were used to do the freeze-thaw cycle test (Figure 2(c)). According to the meteorology observational data of Lanzhou, the freezing temperature of soil samples was set to -20°C , and the melting temperature was set to 20°C . According to the test results of Zhen et al. [29], the soil can be completely frozen after freezing for 4 hours at -20°C . Therefore, in this freeze-thaw cycle

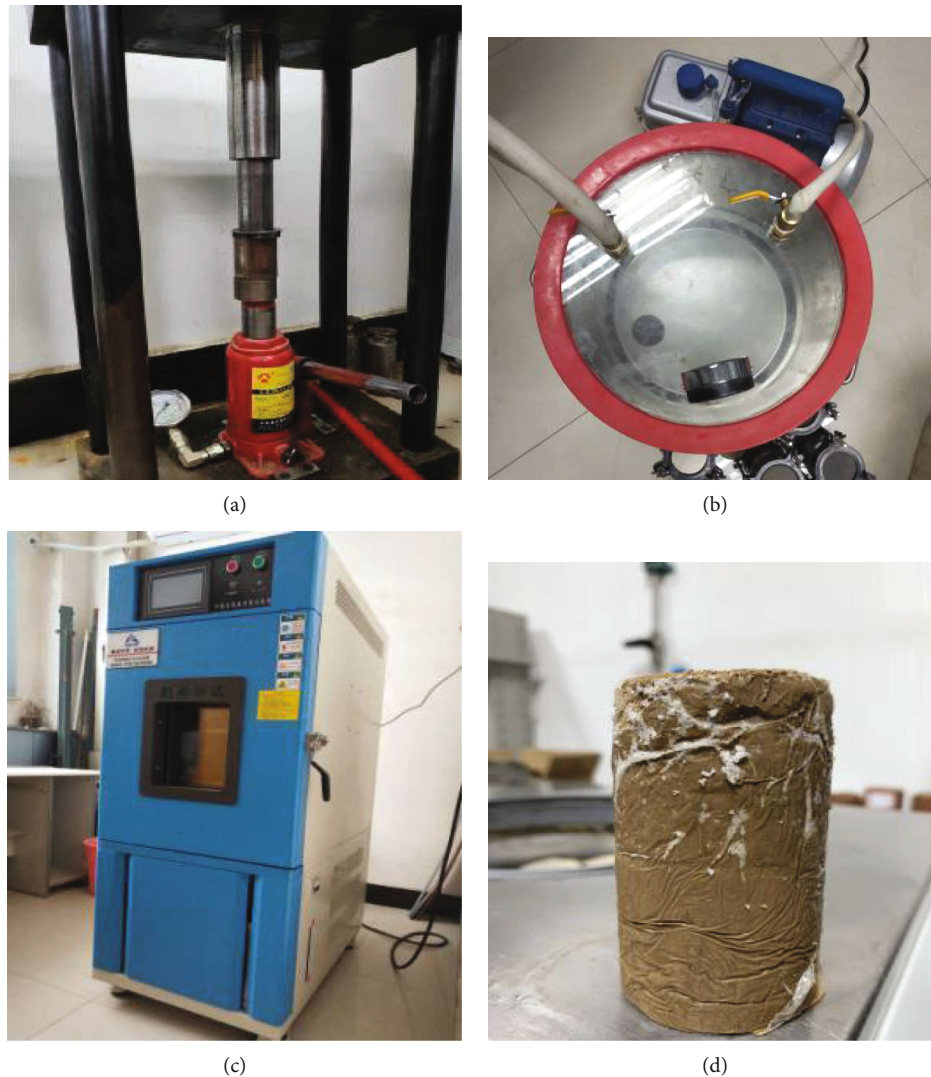


FIGURE 2: Sample preparation and freeze-thaw cycle test: (a) static pressure at both ends to prepare samples; (b) saturation device; (c) freeze-thaw cycle device; (d) sample after freeze-thaw cycle.

test, one freeze-thaw cycle is 12 hours, and the freeze-thaw cycle is 6 hours, respectively. During the test, the soil is frozen in multiple directions without adding water. Studies have shown that freeze-thaw cycles have obvious effects on soil in a short period of time, and the effects become stable after a long period of time [30]. Therefore, four short-term cycles of 1, 4, 7, and 10 are set, and only 40 long-term cycles are set. The sample after freeze-thaw cycle test is shown in Figure 2(d).

2.2.3. Dynamic Triaxial Test. A dynamic triaxial and torsional shear testing system typed WF-12440 was used for the dynamic triaxial test, as shown in Figure 3(a). After completing the freeze-thaw cycle of the soil sample in the LK-120G test box, according to the standard for soil test method (GB/T 50123-2019), the isotropic consolidation mode was adopted to consolidate the samples; the confining pressure in the triaxial tests of this study is uniformly

200 kPa, as shown in Figure 3(b). After the consolidation of the samples was stable, the dynamic triaxial test was carried out by the method of multiloading on one sample. The test was carried out under the condition of consolidated undrained, and the cyclic load was constant-amplitude sinusoidal load with the frequency of 1 Hz [27], and each stage was loaded 10 times for a total of 10 levels. The minimum axial pressure of each specimen is 5 kPa. For the specimens under the freeze-thaw cycles of 0, 1, 4, 7, 10, and 40, the maximum axial pressure in the triaxial tests is 35 kPa, 32 kPa, 38 kPa, 39 kPa, 36 kPa, and 36 kPa, respectively.

2.2.4. SEM Test. The sample after the freeze-thaw cycle is fully freeze-dried with a vacuum freeze-drying apparatus, and the soil sample is gently broken by hand after standing at room temperature. The smooth natural surface was selected. The bottom of the selected sample was ground flat and thin with sandpaper, and the sample was prepared into

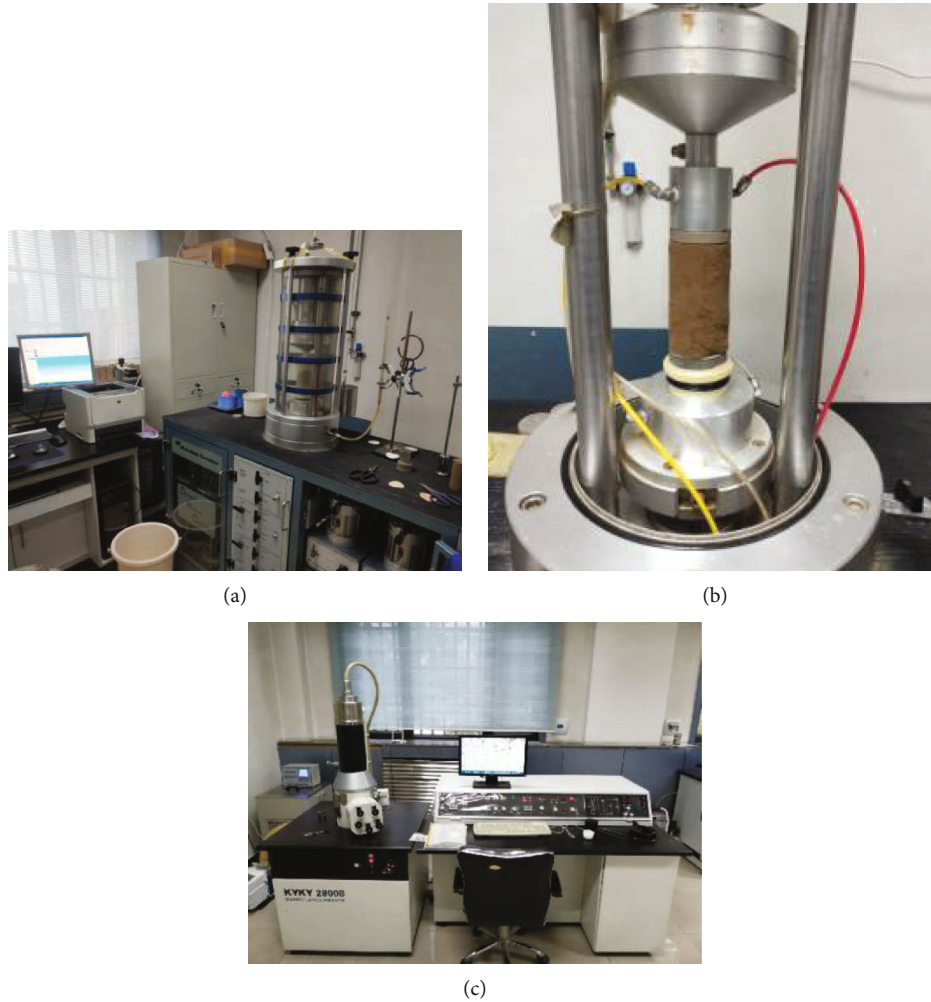


FIGURE 3: Dynamic triaxial test and scanning electron microscope test: (a) WF-12440 dynamic triaxial-torsion shear test system; (b) Test Bench; (c) KYKY2800B-scanning electron microscope.

a square sheet of $10\text{ mm} \times 10\text{ mm} \times 2\text{ mm}$ finally. Then, the section was fixed on the sample holder with conductive glue and put into the ion sputtering equipment for spray gold, making the surface of the sample conductive and easy to image. Then, the scanning electron microscope test was carried out using an equipment typed KYKY-2800B, as shown in Figure 3(c). The multiple shooting was 50, 100, 200, 400, 500, and 800 times, respectively. To ensure that microstructure images have a high accuracy, including enough information, 6 to 8 photos were taken at each magnification.

2.2.5. Acquisition of Microstructural Parameters. The acquisition of the microstructural parameters of the soil relies on the Pores and cracks analysis system (PCAS) [31]. The system can pick up basic microstructural parameters such as the apparent porosity, pore number, and average pore area and statistical calculation parameters such as pore probability entropy, average form coefficient, and fractal dimension through binary processing and vectorization treatment of SEM images.

3. Experiment Results and Analyses

3.1. Dynamic Stress-Dynamic Strain Curves. According to the dynamic triaxial test, the $\sigma_d \sim \varepsilon_d$ curves of the saturated loess after different freeze-thaw cycles are drawn and shown in Figure 4.

It can be seen from Figure 4 that the relationship of $\sigma_d \sim \varepsilon_d$ still obeys the Hardin-Drnevich hyperbolic model [32] after the saturated loess undergoes multiple freeze-thaw cycles, and the dynamic strain increases nonlinearly with the increase of dynamic stress. After one freeze-thaw cycle, the dynamic strain is significantly larger than that of the unfreeze-thaw remolded loess under the condition of the same dynamic stress, the $\sigma_d \sim \varepsilon_d$ curve drops, and the strain weakens. After 4 freeze-thaw cycles, the dynamic strain is greatly reduced compared with the dynamic strain after 1 cycle and is smaller than the dynamic strain after the unfreeze-thaw cycle under the condition of the same dynamic stress. The $\sigma_d \sim \varepsilon_d$ curve rises significantly. After 4 cycles, the dynamic strain decreases with the increase of

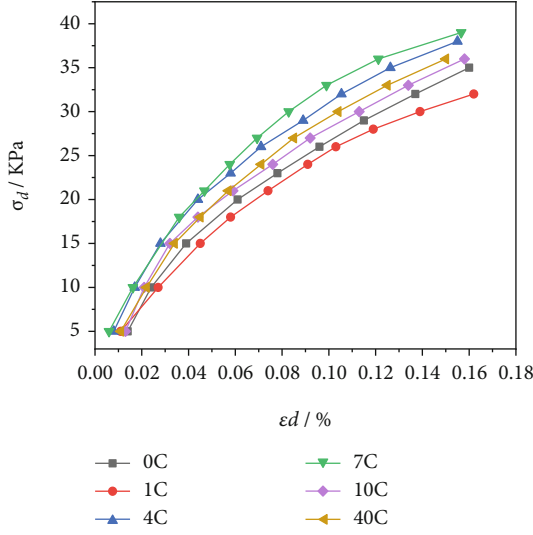


FIGURE 4: $\sigma_d \sim \varepsilon_d$ curves of saturated loess after freeze-thaw cycles.

cycles under the same dynamic stress, and the structural stability is significantly enhanced under external dynamics. After 7 cycles, the $\sigma_d \sim \varepsilon_d$ curve continues to rise. After 10 cycles, the $\sigma_d \sim \varepsilon_d$ curve decreases compared with the $\sigma_d \sim \varepsilon_d$ curve after 7 cycles, but it is still higher than the $\sigma_d \sim \varepsilon_d$ curve of unfreeze-thaw saturated loess. The $\sigma_d \sim \varepsilon_d$ curve after 40 cycles is between the $\sigma_d \sim \varepsilon_d$ curve after 10 cycles and the $\sigma_d \sim \varepsilon_d$ curve after 4 cycles. It can be seen that after the saturated remolded loess undergoes freeze-thaw cycle, the dynamic stability of the soil structure decreases first and then increases significantly, reaches a peak after 7 freeze-thaw cycles, and then gradually decreases after 10 cycles.

The hyperbolic model proposed by Hardin and Drnevich is shown in

$$\sigma_d = \frac{\varepsilon_d}{a + b\varepsilon_d}. \quad (1)$$

The definition of dynamic elastic modulus is shown in

$$E_d = \frac{\sigma_d}{\varepsilon_d}. \quad (2)$$

According to formula (1) and formula (2),

$$\frac{1}{E} = a + b\varepsilon_d, \quad (3)$$

where σ_d is the axial dynamic stress, ε_d is the axial dynamic strain, E_d is the dynamic elastic modulus, a is the reciprocal $1/E_d$ of the corresponding dynamic elastic modulus when $\varepsilon_d = 0$, that is, the reciprocal of the initial dynamic elastic modulus $E_{d \max}$, and b is the slope of the $1/E_d \sim \varepsilon_d$ curve, as shown in Figure 5, which represents the reciprocal of the maximum dynamic stress amplitude $\sigma_{d \max}$.

The parameters a and b and the correlation coefficient R of testing curves are shown in Table 2. It can be seen from Table 2 that the $1/E \sim \varepsilon_d$ curve has a good linear fit-

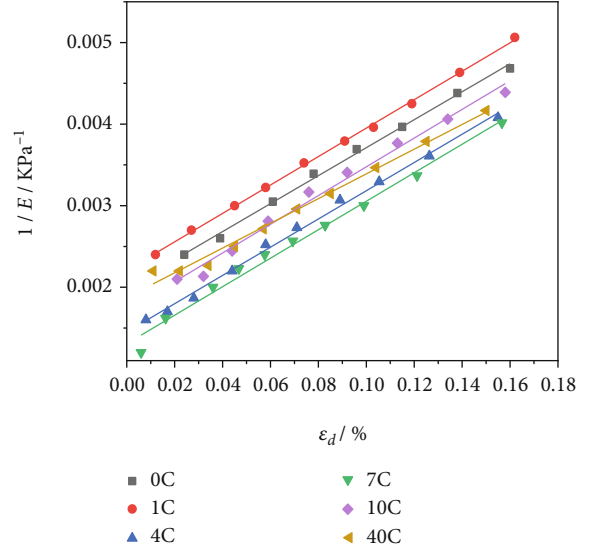


FIGURE 5: $1/E \sim \varepsilon_d$ curves of saturated loess after freeze-thaw cycles.

ting relationship and the freeze-thaw effect has an obvious influence on the parameter a of the hyperbolic model of saturated remolded loess. The maximum dynamic elastic modulus first decreases and then increases with the increase of freeze-thaw cycles, and the parameter b changes little before 10 freeze-thaw cycles, indicating that the slope of the $1/E \sim \varepsilon_d$ curve changes little and decreases after 40 cycles.

3.2. Dynamic Shear Modulus and Damping Ratio. Formula (4) shows the relations between the dynamic shear modulus G_d and dynamic elastic modulus E_d . Formula (5) shows the relation between the dynamic shear strain γ_d and dynamic strain ε_d :

$$G_d = \frac{E_d}{2(1 + \mu)}, \quad (4)$$

$$\gamma_d = (1 + \mu)\varepsilon_d, \quad (5)$$

where μ is Poisson's ratio.

The damping ratio D of soil is calculated by the dynamic stress-dynamic strain hysteresis curve [32, 33], as shown in Figure 6 and formula (6). Where ΔF is the area bounded by the hysteretic curve, F is the area of the triangle AOB.

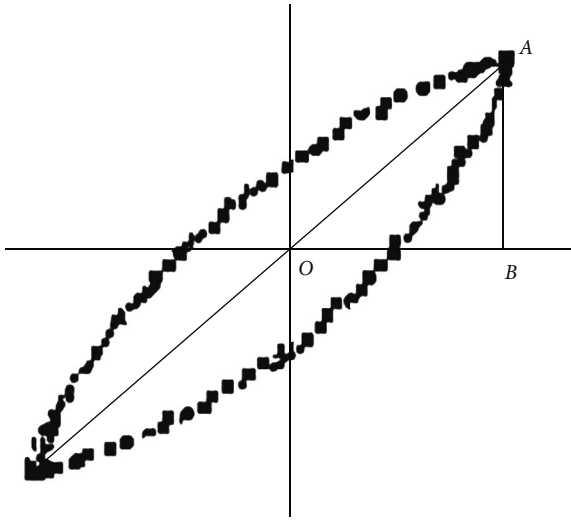
$$D = \frac{1}{4\pi} \frac{\Delta F}{F}. \quad (6)$$

According to formulas (4) and (5), the dynamic shear modulus, dynamic shear strain, and damping ratio are calculated. The $G_d \sim \gamma_d$ curve and $D \sim \gamma_d$ curve are shown in Figures 7 and 8.

The dynamic shear modulus is an important parameter to represent the ability of soil to resist shear deformation. As shown in Figure 7, the dynamic shear modulus of the saturated loess decreases nonlinearly with the increase of dynamic shear strain after different freeze-thaw cycles. After

TABLE 2: Hyperbolic model parameters.

Cycles	Parameters		R
	a	b	
0	0.0020	0.01714	0.995
1	0.00221	0.01743	0.990
4	0.00145	0.01731	0.995
7	0.00131	0.01747	0.990
10	0.00171	0.01767	0.985
40	0.00167	0.01664	0.994

FIGURE 6: Calculation method of the damping ratio D .

the saturated remolded loess undergoes one freeze-thaw cycle, the dynamic shear modulus decreases, due to the volume expansion of water after freezing, the cementation between the particles is destroyed, the skeleton is unstable, and the structural stability is reduced. After 4 freeze-thaw cycles, the dynamic shear modulus of saturated loess increases significantly and reaches the maximum after 7 freeze-thaw cycles, which indicates that when the number of freeze-thaw cycles increases from 1 to 7, the stability of soil structure is significantly improved and the resistance capacity to deformation is improved; that is to say, the frost-heaving stress and water migration force have a certain compaction effect on the soil, reducing the deformation space of the particle skeleton, resulting in the obvious increase of dynamic shear modulus. After the saturated loess undergoes 10 and 40 freeze-thaw cycles, its dynamic shear modulus decreases compared with that of 7 cycles, but it is still greater than the dynamic shear modulus of remolded loess and under the same dynamic strain level. The difference between the dynamic elastic modulus of saturated loess with 10 freeze-thaw cycles and 40 freeze-thaw cycles is small, indicating that after long-term freeze-thaw cycles, the dynamic shear modulus of saturated loess tends to be stable and the dynamic stability of the soil is enhanced compared with saturated loess without freezing and thawing.

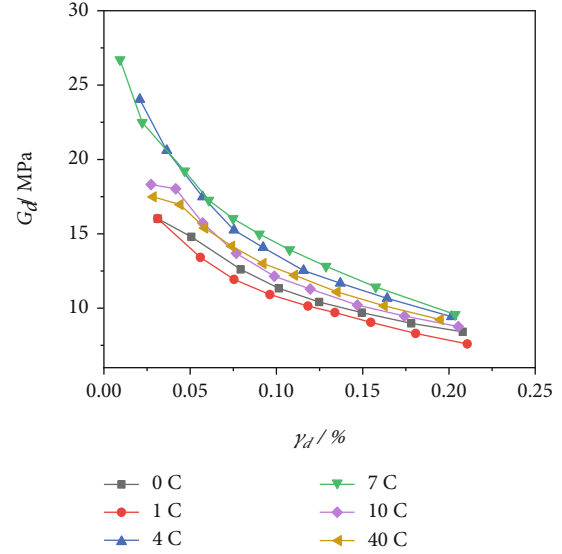


FIGURE 7: Curve of dynamic shear modulus versus dynamic shear strain after freeze-thaw cycles.

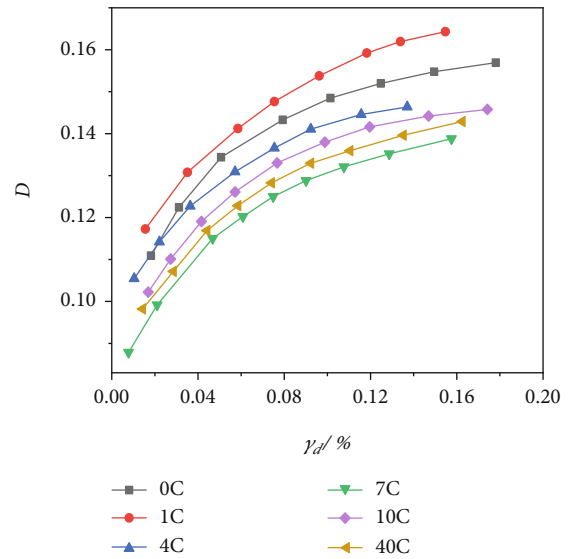


FIGURE 8: Damping ratio-dynamic shear strain curves after freeze-thaw cycles.

The damping ratio of the soil reflects the property of energy loss due to the internal resistance of the soil under dynamic load, representing the influence of the viscosity of the soil on its dynamic constitutive relationship. It can be seen from Figure 8 that the damping ratio of saturated loess increases nonlinearly with the increase of dynamic shear strain after the freeze-thaw cycle. When the dynamic shear strain is less than 0.1%, the damping ratio increases rapidly, and when the dynamic shear strain is more than 0.1%, the damping ratio increases gently. The number of freeze-thaw cycles has a significant effect on the damping ratio of saturated loess. Because of the increase in the pore size of the soil, after one freeze-thaw cycle, the particle connections tend to loosen, the probability of friction between particles

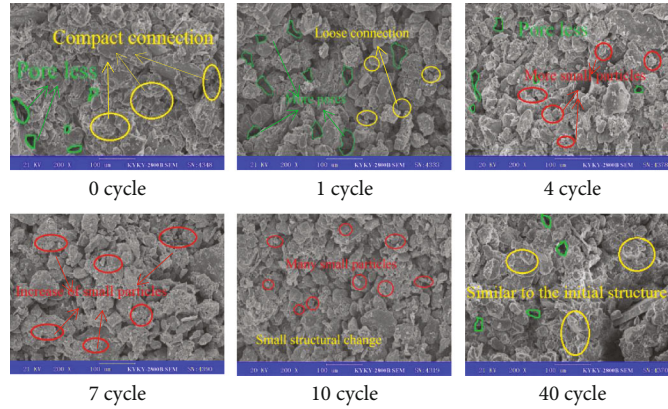


FIGURE 9: SEM image before and after freeze-thaw cycles (200x).

increases, the energy consumption increases, and the damping increases significantly compared with that of unfreeze-thaw remolded loess. With the increase of the number of freeze-thaw cycles, the damping ratio continued to decrease from 1 freeze-thaw cycle to 7 freeze-thaw cycles and increased after 10 cycles. After 40 freeze-thaw cycles, the damping ratio increases again and tends to be stable generally, but it is still smaller than the damping ratio of unfreeze-thaw saturated loess and saturated loess after 4 freeze-thaw cycles under the condition of the same dynamic strain, indicating that the freeze-thaw cycle makes the saturated loess grain refinement and aggregation, the frictional energy consumption between particles becomes weakened, and the whole structure of the soil develops towards homogenization and densification.

3.3. Microstructure. The SEM images with a magnification of 200 times are selected for qualitative analysis, as shown in Figure 9. The PCAS was used to process SEM images with a magnification of 500 times, the quantitative parameters of microstructure were extracted, and the microstructure changes of saturated loess after different freeze-thaw cycles were analyzed.

As shown in Figure 9, the unfrozen remolded loess particles are large, with close arrangement and connection among the particles, with few pores and mainly small pores. There are natural microcracks and microcracks in the particles, and liquid water fills the pores after back pressure saturation. After one freeze-thaw cycle of saturated soil, the soil structure changed significantly, the macropores increased, and the contact relationship between particles changed from surface-to-surface contact to point-to-surface contact, the connection was loose, and the soil structure was destroyed. After four cycles, the number of pores decreased obviously, the particles reaggregated, and the soil structure became dense again. After seven and ten freeze-thaw cycles, the small particles increased, but the soil structure did not change obviously. After forty freeze-thaw cycles, a stable structure similar to that of remolded soil can be seen.

Using the Feret diameter to represent the average diameter h of particles [31]. According to the study of Mu et al. [18], $h \leq 5 \mu\text{m}$ was defined as microparticles, $5 \mu\text{m}$

$\leq h \leq 10 \mu\text{m}$ was defined as small particles, $10 \mu\text{m} \leq h \leq 20 \mu\text{m}$ was defined as medium particles, and $h \geq 20 \mu\text{m}$ was defined as large particles. The ratio of the pore area to the area of the SEM photograph representing the change of particle size and porosity was obtained by statistical analysis, as shown in Figures 10 and 11.

It can be seen from Figures 10 and 11 that after one cycle, the number of large and medium particles decreases slightly, the number of micro- and small particles increases slightly, and the apparent porosity increases sharply, indicating that the soil skeleton is deformed by compressing and the pore is expanded during one cycle. There are no obvious damage and cracking in the large and medium particles, and the freeze-thaw action only causes the frost movement of the soil. The microstructure is presented as the number of pores increases, the size increases, the structure is loose, and frost heave occurs. After four freeze-thaw cycles, the number of large and medium particles decreases significantly, the number of micro- and small particles increases, and the porosity decreases significantly; after four cycles, the original structure of the remolded loess is completely destroyed and the microcracks and microfissure of soil particles expand and penetrate, the structure of large particles is damaged and broken, the broken particles fall and fill in the pores, and the large pores are filled and closed. It can be seen that from the SEM photo with a magnification of 200 times after 4 cycles, the surface of large particles is attached with broken micro- and small particles, the surface is rough, the size of soil particles tends to be uniform, and the compactness of soil increases, manifesting that the soil particles are gathered at this stage and the structure develops towards stability. After 7 cycles, the porosity decreases and the number of large particles still decreases, but the number of medium particles increases, and the number of microparticles slightly decreases, illustrating that after 7 cycles, the micro- and small particles agglomerate occurs due to the frost heaving pressure, water migration force, and van der Waals force, the particle volume and bonding strength increase, and the integrity of soil increases. After 10 cycles, the porosity increases slightly, large and medium particles continue to break, and the number of micro- and small particles increases compared with that after 7 cycles. After 40 cycles,

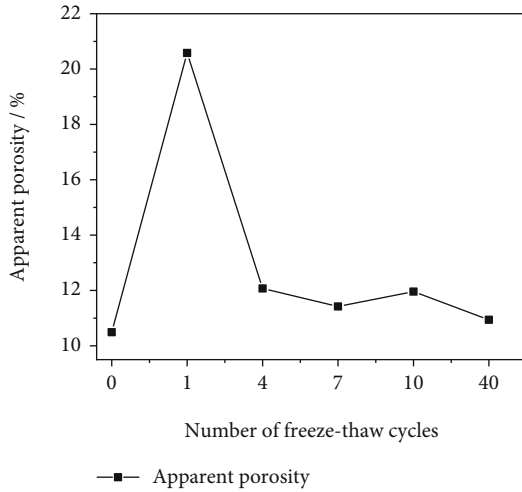


FIGURE 10: Change of particle size after different freeze-thaw cycles.

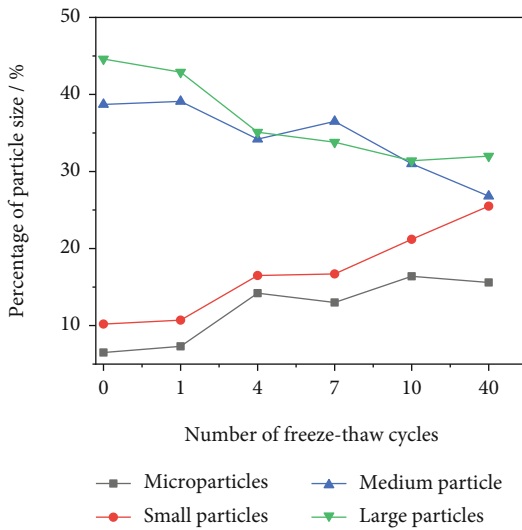


FIGURE 11: Change of apparent porosity after different freeze-thaw cycles.

the soil structure changes little, the uniformity of particle size reaches the best, the connection between particles is close, and the soil structure is stable. Compared with the unfreeze-thaw remolded soil, the density of soil structure is similar, and the particles are mainly surface-to-surface contact. However, after 40 cycles, the particles are smaller and more uniform and the integrity is better.

The micromechanical morphology of pores is an important aspect that affects the loess structure. The fractal dimension of pores can quantitatively describe the complexity of pores [34]. The changes of fractal dimension of soil pores and particles after freeze-thaw cycles are shown in Figure 12. The saturated loess undergoes different numbers of freeze-thaw cycles; the fractal dimensions of particles and pores both show a decreasing trend, of which the pores are faster than that of the particles. Under the action of force in the freeze-thaw cycle, the irregular edges and corners of soil particles are easy to be cut off,

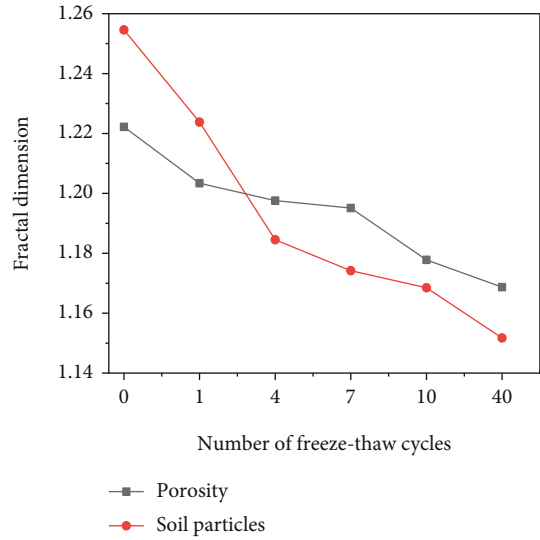


FIGURE 12: Change of fractal dimension after different freeze-thaw cycles.

the roundness of the particles increases, the surface undulation degree decreases, the particle shape tends to be regular, and the complexity of pore shape formed by particle framework decreases. After freeze-thaw cycles, the simplification of particle and pore shape makes the particles have better connection, and the structural integrity and stability are enhanced [25].

The probability entropy (H_m) can reflect the orientation of loess particles and pores arrangement. The larger the probability entropy is, the worse the orderliness and orientation of the pores arrangement are. The range of H_m is (0~1). The orientation arrangement is stronger when the H_m is smaller [35]. The change of probability entropy of saturated loess pores and particles after different numbers of freeze-thaw cycles is shown in Figure 13.

As shown in Figure 13, With the increase of freeze-thaw cycles, the probability entropy of particles and pores first increases and then decreases. After one freeze-thaw cycle and four freeze-thaw cycles, the probability entropy of pores and particles is the largest, respectively. After one freeze-thaw cycle, the original arrangement of pores and particles is destroyed, the arrangement direction is disordered, and the structure is disordered. With the increase of cycle times, due to the reorganization of soil structure, the number of pores is reduced and the water migration channel is gradually stable, the arrangement of particles and pores tends to be oriented, the probability entropy decreases, and the stability of soil is enhanced.

4. Discussion

Based on the above analysis results after several freeze-thaw cycles, the dynamic performance of saturated loess is stronger than that of unfreeze-thaw remolded loess in a closed environment without water recharge, and the soil structure is more stable and denser.

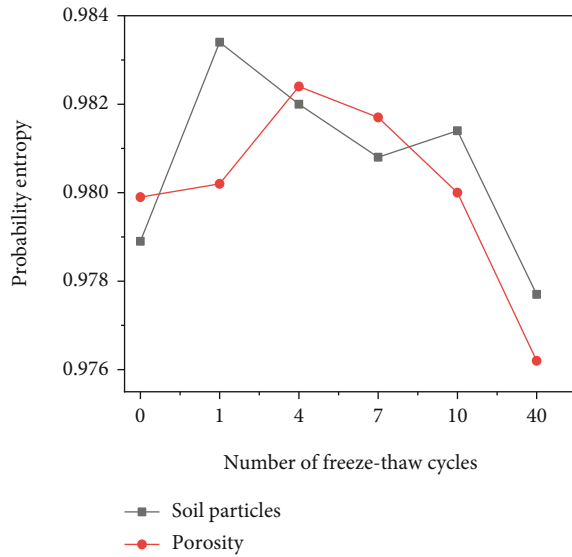


FIGURE 13: Change of probability entropy after different freeze-thaw cycles.

Freeze-thaw action is a kind of strong weathering. The transformation process from water to ice strongly changes the structure of soil and destroys the connection and arrangement of original particles. At the same time, in the process of freezing, the surface layer of the soil is first frozen by cold, then the binding water film has frozen cracks, the temperature gradient and electric field gradient are generated inside, and the water migration force reacts on the soil structure, which causes further damage. In addition, as a high dispersibility multiminer aggregate, the deformation of each individual mineral in the soil is different in the process of temperature change, which shows the anisotropy of thermal and physical properties of soil skeleton [36, 37]. Therefore, after the freeze-thaw cycle, the saturated loess first shows the expansion of pores, the dispersed particles, and disordered arrangement, and the whole structural stability decreases, and its dynamic stability decays to a certain extent.

After many freeze-thaw cycles tested on soil, soil particle split only occurs in the relatively coarse particle size under the freeze-thaw action, whereas fine particles will agglomerate due to the effect of the electric double layer [38]. Based on the powder-sized microscopic analysis of the overburden soil after multiple freeze-thaw cycles, the powder is an aggregate with fine sand as the core and the aggregate is wrapped by clay particles; the aggregation process of soil particles is an associated product of the splitting process during freeze-thaw cycles [36]. Therefore, after the freeze-thaw cycle, the larger particles in the soil develop to smaller particle size because of fracturing, and the micro- and small particles develop to larger particle size because of agglomeration, which leads to the enrichment of soil particles in a certain size eventually. After the destruction of the soil structure, the particles of saturated loess are damaged and cracked. Under the action of van der Waals force and hydrogen bond, the particles are condensed and agglomerated, the water migration causes the dehydration

of soil particles, the wedging action of ice interlayer causes the compaction of soil, and at the same time, a recrystallization process of minerals may happen under the substantial stress, comparing with the “cold hammer welding,” the strength of particle cementation increases. In this paper, the compaction cementation is the most obvious in seven freeze-thaw cycles, and the dynamic stability of soil is the strongest at this time. After more than 7 freeze-thaw cycles, the particle breakage and agglomeration of the soil continue to develop during the continuous freeze-thaw process. Although the dynamic stability of the soil is weakened to some extent, it is still larger than that of the remolded loess overall. Because of the action of remodeling and saturation, the initial structure of loess is completely destroyed, and the freeze-thaw action leads to the increase of micro- and small particles in the soil. The agglomeration and cementation caused by the electric double layer play a major role to make the connection between fine particles closer and the structural strength stronger, which leads to the weakening of the dynamic vulnerability of loess after long-term freeze-thaw cycles. In addition, existing studies also have the situation that the mechanical strength of the soil increases after the freeze-thaw cycle. Liu et al. [39] found that under the action of freeze-thaw cycle, the mechanical properties of silty clay with low water content were weakened, and when the water content increased to the plastic limit, the freeze-thaw cycle effect was strengthened; Hu et al. believed that due to water redistribution after the freezing-thawing cycle, the mechanical strength in the region where the water content decreased increased, and the mechanical strength in the region where the water content increased decreased, the strength variation amplitude of the two regions is different, which will cause the change of the overall failure strength of the soil. The mechanical strength of the soil may be strengthened, weakened, or unchanged, and the high water content is conducive to the strengthening effect. Dong et al. [11] believed that water loss in soil after freezing-thawing cycle would cause strengthening phenomenon. Qi et al. and Song et al. [40, 41] found that freezing-thawing cycles have both strengthening and weakening effects on soils with different dry bulk densities; they believe that this is caused by the overconsolidation effect of negative pore water pressure on soil during freezing. Oztas and Fayetorbay [42] found that when the freeze-thaw cycle increased from 3 to 6 times, the mechanical properties of soil with high water content strengthened. Viklander [43] found that the cohesion and early consolidation pressure of soils with low density increased after the freeze-thaw cycle. Zhao [44] found that aeolian soil has a self-healing effect under the action of freeze-thaw cycles. After a long period of freeze-thaw cycles, the structure and mechanical strength of aeolian soil are similar to those before freeze-thaw cycles. Similarly, in this paper, after 40 freeze-thaw cycles, the structure of saturated loess is similar to that of dynamic shear modulus and unfrozen freeze-thaw. It can be seen that two opposite effects, deterioration and strengthening, may occur in the mechanical properties of soil after freezing-thawing cycle [45]. The reason for this difference and the variation law of both with water content have not been agreed; further research is needed.

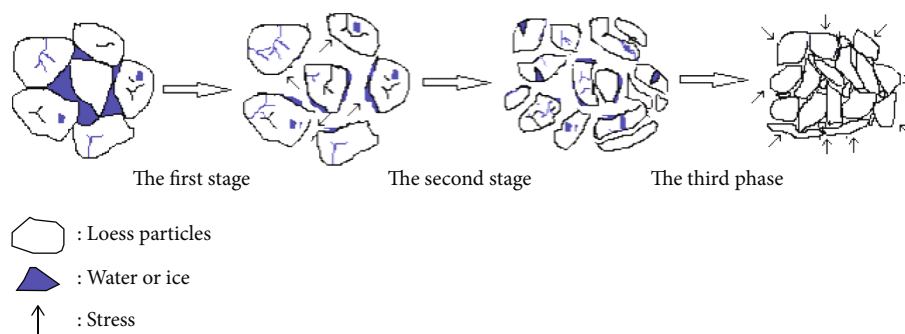


FIGURE 14: Schematic diagram of microstructure changes under the action of freezing and thawing of saturated loess.

It can be seen from the above analysis that the structural change of saturated remolded loess under freeze-thaw cycle mainly goes through three stages, as shown in Figure 14. The first stage is the frost heaving deformation failure of the soil skeleton. It is mainly about that during the first freeze-thaw cycle, the variation characteristics of the microstructure are cementation fracture between particles, expansion of pores, and complete destruction of the original structure. The dynamic properties are strain weakening, dynamic shear modulus decreasing, and damping ratio increasing. The second stage is the damage and rupture of large and medium particles, and this stage is mainly between 1 and 4 freeze-thaw cycles. The variation characteristics of microstructure are that the large and medium particles decrease significantly, the roundness of the particle improves, the degree of particle homogenization increases, the damping ratio decreases, the dynamic shear modulus increases significantly, the influence of freeze-thaw cycles on soil changes from weakening to strengthening, and the dynamic characteristics are significantly enhanced compared with those of unfreeze-thaw soil. The third stage is the compaction and reorganization of soil structure. The typical performance is that after seven freeze-thaw cycles, the characteristics of the microstructure are micro- and fine particles that agglomerate to medium particles, the soil structure is uniform and dense, and the integrity is significantly increased [46, 47]. The dynamic characteristics of this stage reach the best.

5. Conclusion

This work provides the dynamic behaviors of the saturated compacted loess after freezing-thaw cycles and correlative characteristics of microstructures. Based on these results, several conclusions could be drawn as follows:

- (1) After the saturated remolded loess undergoes one freeze-thaw cycle, the soil strain weakens and the damping ratio increases. After four freeze-thaw cycles, the soil strain strengthens. After seven freeze-thaw cycles, the dynamic shear modulus reaches the maximum and the damping ratio is the minimum. The dynamic performance of saturated remolded loess is enhanced after multiple freeze-thaw cycles
- (2) The influence of freeze-thaw cycles on the structure of saturated remolded loess is obvious. With the increase of the number of freeze-thaw cycles, the number of large and medium particles decreases, the number of micro- and small particles increases, the apparent porosity decreases, the component develops towards homogenization, the shape complexity of pores and particles decreases, the arrangement tends to be neat, and the integrity of soil structure increases
- (3) The structural changes of saturated loess under freeze-thaw cycles are affected by destruction and agglomeration, which can be divided into three stages: fracture and expansion of skeleton cementation, damage, crushing and aggregation of the particles and compaction and reorganization of soil structure. Besides, the saturation significantly accelerates the influence of freeze-thaw cycles on the structure of soil

Data Availability

The data used to support the findings of this study are included within the article.

Conflicts of Interest

The authors declare that they have no competing interests.

Authors' Contributions

Qian Wang contributed to conceptualization, dynamic tri-axial tests, data analyzing, and the result and discussion parts of this draft. Fuqiang Liu contributed to sample collection, laboratory tests, data analyzing, and other parts of this manuscript. Xiumei Zhong contributed to project administration, SEM tests, and data analysis. Zhongnan Gao contributed to laboratory tests and data curation. Shouyun Liang helped us to review and revise the text of this paper. Yuxin Liang participated in some sample collections and laboratory tests. Fuqiang Liu as co-first author.

Acknowledgments

This study was supported in part by the Special Fund for Innovation Team, Gansu Earthquake Agency (Grant No. 2020TD-01-01); the Funding of Science for Earthquake Resilience (Grant Nos. XH20057 and XH21034); the National Natural Science Foundation of China (Grant Nos. 51778590 and 51408567); the grant of the Fundamental Research Funding for the Institute of Earthquake Forecasting, China Earthquake Administration (Grant No. 2018IESLZ06); and the Science and Technology Projects Funding for Lanzhou City (Grant No. 2018-1-123). The authors thank Master Chao Cheng and Xiaowei Xu for their contributions to editing and language modification.

References

- [1] Y. Y. Wang and Z. G. Lin, *The China loess structure features and its physical and mechanical properties*, Science Press, Beijing, 1990.
- [2] I. F. Jefferson, D. Evstatiev, D. Karastanev, N. G. Mavlyanova, and I. J. Smalley, "Engineering geology of loess and loess-like deposits: a commentary on the Russian literature," *Engineering Geology*, vol. 68, no. 3–4, pp. 333–351, 2003.
- [3] Y. Li, W. Shi, A. Aydin, M. A. Beroya-Eitner, and G. Gao, "Loess genesis and worldwide distribution," *Earth-Science Reviews*, vol. 201, article 102947, 2019.
- [4] W. Ma and D. Y. Wang, "Studies on frozen soil mechanics in China in past 50 years and their prospect," *Chinese Journal of Geotechnical Engineering*, vol. 34, no. 4, pp. 625–640, 2012.
- [5] G. Y. Li, W. Ma, Y. H. Mu, F. Wang, S. Z. Fan, and Y. H. Wu, "Effects of freeze-thaw cycle on engineering properties of loess used as road fills in seasonally frozen ground regions, North China," *Journal of Mountain Science*, vol. 14, no. 2, pp. 356–368, 2017.
- [6] Z. W. Zhou, W. Ma, S. J. Zhang, Y. Mu, and G. Li, "Effect of freeze-thaw cycles in mechanical behaviors of frozen loess," *Cold Regions Science and Technology*, vol. 146, pp. 9–18, 2018.
- [7] D. Chang, J. Liu, X. Li, and Q. Yu, "Experiment study of effects of freezing-thawing cycles on mechanical properties of Qinghai-Tibet silty sand," *Chinese Journal of Rock Mechanics and Engineering*, vol. 3, no. 7, pp. 1496–1502, 2014.
- [8] J. L. Qi, W. Ma, and C. X. Song, "Influence of freeze-thaw on engineering properties of a silty soil," *Cold Regions Science and Technology*, vol. 53, no. 3, pp. 397–404, 2008.
- [9] W. Ma, X. Z. Xu, and L. X. Zhang, "Influence of frost and thaw cycles on shear strength of lime silt," *Chinese Journal of Geotechnical Engineering*, vol. 21, no. 2, pp. 23–25, 1999.
- [10] T. L. Wang, Y. J. Liu, H. Yan, and L. Xu, "An experimental study on the mechanical properties of silty soils under repeated freeze-thaw cycles," *Cold Regions Science and Technology*, vol. 112, pp. 51–65, 2015.
- [11] X. H. Dong, A. J. Zhang, and J. B. Lian, "Study of shear strength deterioration of loess under repeated freezing-thawing cycles," *Journal of Glaciology and Geocryology*, vol. 32, no. 4, pp. 767–772, 2010.
- [12] W. Y. Zhang, A. B. Guo, and C. Lin, "Effects of cyclic freeze and thaw on engineering properties of compacted loess and lime-stabilized loess," *Journal of Materials in Civil Engineering*, vol. 31, no. 9, article 04019205, 2019.
- [13] J. Sun, M. S. Gong, and H. Q. Xiong, "Experimental study of the effect of freeze-thaw cycles on dynamic characteristics of silty sand," *Rock and Soil Mechanics*, vol. 41, no. 3, pp. 747–754, 2020.
- [14] S. Zhang, C. A. Tang, X. D. Zhang, Z. C. Zhang, and J. X. Jin, "Cumulative plastic strain of frozen aeolian soil under highway dynamic loading," *Cold Regions Science and Technology*, vol. 120, pp. 89–95, 2015.
- [15] Y. Zheng, W. Ma, and H. Bing, "Impact of freezing and thawing cycles on structure of soils and its mechanism analysis by laboratory testing," *Rock and Soil Mechanics*, vol. 36, no. 5, pp. 1282–1287, 2015.
- [16] W. J. Ye, C. Q. Li, and X. H. Dong, "Study on damage identification of loess microstructure and macro mechanical response under freezing and thawing conditions," *Journal of Glaciology and Geocryology*, vol. 40, no. 3, pp. 546–555, 2018.
- [17] W. K. Ni and H. Q. Shi, "Influence of freezing-thawing cycles on micro-structure and shear strength of loess," *Journal of Glaciology and Geocryology*, vol. 36, no. 4, pp. 922–927, 2014.
- [18] Y. H. Mu, W. Ma, G. Y. Li, and Y. C. Mao, "Quantitative analysis of impacts of freeze-thaw cycles upon microstructure of compacted loess," *Chinese Journal of Geotechnical Engineering*, vol. 33, no. 12, pp. 1919–1925, 2011.
- [19] Q. Wang, X. M. Zhong, Z. N. Gao et al., "Liquefaction behaviors of the saturated loess in Lanzhou City under freezing-thawing conditions," *Chinese Journal of Rock Mechanics and Engineering*, vol. 39, no. S1, pp. 2986–2994, 2020.
- [20] T. X. Wang, S. F. Luo, and X. J. Liu, "Testing study of freezing-thawing strength of unsaturated undisturbed loess considering influence of moisture content," *Rock and Soil Mechanics*, vol. 31, no. 8, pp. 2378–2382, 2010.
- [21] T. F. Hu, J. K. Liu, J. H. Fang, A. H. Xu, and D. Chang, "Experimental study on the effect of moisture content on mechanical properties of silty clay subjected to freeze thaw cycling," *Journal of Harbin Institute of Technology*, vol. 49, no. 12, pp. 123–130, 2017.
- [22] G. Y. Li, F. Wang, W. Ma et al., "Variations in strength and deformation of compacted loess exposed to wetting-drying and freeze-thaw cycles," *Cold Regions Science and Technology*, vol. 151, pp. 159–167, 2018.
- [23] X. S. Mao, Z. J. Hou, and W. N. Wang, "Experimental research on resilient modulus of remolded soil based on water content and freeze-thaw cycles," *Chinese Journal of Rock Mechanics and Engineering*, vol. 28, Supplement 2, pp. 3585–3590, 2009.
- [24] F. Niu, J. Luo, Z. Lin, J. Fang, and M. Liu, "Thaw-induced slope failures and stability analyses in permafrost regions of the Qinghai-Tibet Plateau, China," *Landslides*, vol. 13, no. 1, pp. 55–65, 2016.
- [25] J. Ning, Y. H. Wang, and C. M. Zhang, "Influence of initial water content and freeze-thaw cycles on microstructure of loess," *Science Technology and Engineering*, vol. 18, no. 5, pp. 285–290, 2018.
- [26] Y. Wei, *Analysis of influence of freeze-thaw cycles on physical and mechanical properties of loess with high water content*, Xi'an University of Science and Technology, Xi'an, 2016.
- [27] Q. Wang, J. L. Ma, H. P. Ma, J. Wang, L. M. Wang, and Z. N. Gao, "Dynamic shear modulus and damping ratio of saturated loess," *Chinese Journal of Rock Mechanics and Engineering*, vol. 38, no. 9, pp. 1919–1927, 2019.

- [28] Ministry of Water Resources of the People's Republic of China and GB/T50123-2019, "Standard for geotechnical testing method," China Metrology Publishing House, Beijing, 2019.
- [29] X. Zheng, W. Ma, and H. Bin, "Impact of freezing and thawing cycles on the structures of soil and a quantitative approach," *Journal of Glaciology and Geocryology*, vol. 1, no. 37, pp. 132–137, 2015.
- [30] Y. Q. Su, W. Ma, and X. M. Zhong, "Experimental study of influence of freeze-thaw cycles on dynamic nonlinear parameters of Qinghai-Tibet silty clay," *Chinese Journal of Rock Mechanics and Engineering*, vol. 39, Supplement 1, pp. 1282–1294, 2020.
- [31] C. Liu, B. Shi, J. Zhou, and C. Tang, "Quantification and characterization of microporosity by image processing, geometric measurement and statistical methods: application on SEM images of clay materials," *Applied Clay Science*, vol. 54, no. 1, pp. 97–106, 2011.
- [32] B. O. Hardin and V. P. Drnevich, "Shear modulus and damping in soils: design equations and curves," *Journal of the Soil Mechanics and Foundations Division, ASCE*, vol. 98, no. 7, pp. 667–692, 1972.
- [33] H. B. Seed and I. M. Idriss, *Soil moduli and damping factors for dynamic response analyses*, EERC, Berkely, Calif, 1970.
- [34] M. R. Cox and M. Budhu, "A practical approach to grain shape quantification," *Engineering Geology*, vol. 96, no. 1–2, pp. 1–16, 2008.
- [35] B. Shi, "Quantitative research on the orientation of microstructures of clayey soil," *Acta Geologica Sinica*, vol. 71, no. 1, pp. 36–44, 1997.
- [36] Z. Zhang, W. Ma, and J. L. Qi, "Structure evolution and mechanism of engineering properties change of soils under effect of freeze-thaw cycle," *Journal of Jilin University: Earth Science Edition*, vol. 43, no. 6, pp. 1904–1914, 2013.
- [37] Y. Zheng, W. Ma, and H. Bin, "Impact of freezing and thawing cycles on the structures of soil and a quantitative approach," *Rock and Soil Mechanics*, vol. 37, no. 1, pp. 132–137, 2015.
- [38] E. J. Chamberlain and A. J. Gow, "Effect of freezing and thawing on the permeability and structure of soils," *Engineering Geology*, vol. 13, no. 1-4, pp. 73–92, 1979.
- [39] H. B. Liu, H. Z. Zhang, and J. Wang, "Effect of freeze-thaw and water content on mechanical properties of compacted clayey soil," *Rock and Soil Mechanics*, vol. 29, no. 1, pp. 158–164, 2018.
- [40] J. L. Qi and W. Ma, "Influence of freezing-thawing on strength of overconsolidated soils," *Chinese Journal of Geotechnical Engineering*, vol. 28, no. 12, pp. 2082–2086, 2006.
- [41] C. X. Song, J. L. Qi, and F. Y. LIU, "Influence of freeze-thaw on mechanical properties of Lanzhou loess," *Rock and Soil Mechanics*, vol. 29, no. 4, pp. 1077–1086, 2008.
- [42] T. Oztas and F. Fayetorbay, "Effect of freezing and thawing processes on soil aggregate stability," *Catena*, vol. 52, no. 1, pp. 1–8, 2003.
- [43] P. Viklander, "Permeability and volume changes in till due to cyclic freeze-thaw," *Canadian Geotechnical Journal*, vol. 35, no. 3, pp. 471–477, 1998.
- [44] L. Zhao, *Analysis of effect of aelian soil self-healing on the dynamical property under freeze-thaw*, Liaoning Technical University, 2012.
- [45] X. Zhang, E. Zhai, Y. Wu, D. Sun, and Y. Lu, "Theoretical and numerical analyses on hydro-thermal-salt-mechanical interaction of unsaturated salinized soil subjected to typical unidirectional freezing process," *International Journal of Geomechanics*, vol. 21, no. 7, article 04021104, 2021.
- [46] Z.-Q. Zhang, Q.-B. Wu, M.-T. Hou, B.-W. Tai, and Y.-K. An, "Permafrost change in Northeast China in the 1950s-2010s," *Advances in Climate Change Research*, vol. 12, no. 1, 2021.
- [47] Z. Q. Zhang, Q. B. Wu, G. Jiang, G. Siru, C. Ji, and L. Yongzhi, "Changes in the permafrost temperatures from 2003 to 2015 in the Qinghai-Tibet Plateau," *Cold Regions Science and Technology*, vol. 169, article 102904, 2020.